Comitato Nazionale per L'Energia Nucleare
ISTITUTO NAZIONALE DI FISICA NUCLEARE

Sezione di Padova

INFN/BE-68/11
11 Ottobre 1968

L. Taffara and V. Vanzani: ON THE REACTION MECHANISM IN HEAVY-ION NEUTRON TUNNELLING PROCESSES. -

Reparto Tipografico
dei Laboratori Nazionali di Frascati

Istituto Nazionale di Fisica Nucleare
Sezione di Padova

INFN/BE - 68/11
11 Ottobre 1968

L. Taffara(x) and V. Vanzani: ON THE REACTION MECHANISM IN HEAVY-ION NEUTRON TUNNELLING PROCESSES. -

SUMMARY. -

Feynman diagram techniques are applied to the heavy-ion neutron transfer reactions at energies below the Coulomb barrier. A triangular graph mechanism is proposed in order to describe the three-body rearrangement process. The effects of the off--energy-shell core-core Coulomb scattering and the initial and final state interactions are investigated and compared with those treated in the TMA and DWBA approaches.

1. - INTRODUCTION. -

As it is well known, the three-body rearrangement scattering problem, involved in the heavy-ion neutron transfer processes, represents a basic step in understanding the heavy-ion interaction dynamics. This explains the considerable theoretical interest devoted to these reactions. The distorted-wave Born approximation (DWBA), the molecular state approximation (MSA) and the T-matrix approximation (TMA) can be considered the main attempts to solve this rearrangement problem.

It has been shown that the MSA approach gives a transition amplitude formally identical to the DWBA theory and, therefore, can be considered as a method that provides an alternative derivation of the DWBA matrix element(1).

On the contrary, non trivial differences exist between the TMA and the DWBA (or the equivalent MSA) theories; in fact they represent different approximations of the three-body problem, and, therefore, different reaction mechanisms. As a consequence, the nuclear structure and the spectroscopic information obtained from these theories could not be reliable, in spite of the satisfactory agreement with the experimental cross section behaviour(2).

In order to understand the differences between the DWBA and the TMA approaches and to describe correctly heavy-ion transfer processes, one should apply the general methods, which have recently been introduced to solve the three-body scattering problems. Unfortunately, these techniques have not been developed sufficiently for practical purposes in nuclear reaction problems.

However, one can obtain some new insight into the general questions involved in the heavy-ion rearrangement reactions, by extending to these processes the non-relativi

---

(x) - Istituto di Fisica dell'Università - Lecce. Istituto Nazionale di Fisica Nucleare - Sottosezione di Bari.

stic Feynman-diagram techniques, which have been proved useful in the analysis of direct interactions as in the (p, d), (d, t), (He^3, α) reactions[3÷8].

The purpose of this paper is to construct the reaction amplitude on the basis of a suitable diagram (to which we refer in the following as "fundamental diagram") which describes the three-body rearrangement mechanism and does not take into account the initial and final state interactions. These latter will then be represented by means of graphs containing the exact initial and final state scattering amplitude[7].

Among the possible heavy-ion transfer processes, the low energy neutron transfer reaction, usually called neutron "tunnelling", represents an interesting tool for a critical study on the possibility of obtaining reliable information about reaction mechanism and nuclear structure. In fact, the description of the neutron tunnelling process is a fairly "clean" problem, because: (a) nuclear and Coulomb interactions appear separated in the reaction amplitude, (b) Coulomb potential dominates the scattering problem and it is accurately known, while the unknown short-range part of the nuclear wave functions affects very little the angular and energetic dependence of the amplitude (but in an important way the over-all normalization). For these reasons the cross section should not depend sensitively on the several parametrizations which complicate higher energy processes[1]. However, because of the many-body aspects of the nuclear particles and of the off-energy--shell Coulomb scattering amplitude contributions, the tunnelling process does not represent a trivial problem.

In applying the non-relativistic Feynman-graph tecniques to the heavy-ion interaction processes, the usual criteria of choosing the fundamental graphs should now be modified by the relevant role of the Coulomb interactions[3, 8÷10].

In Sect. 2 we introduce the essential features of the Feynman-diagram approach (FDA) for tunnelling processes. Section 3 is devoted to the triangular graph which describes the three-body rearrangement scattering. After some short considerations on the possible forms of the off-energy-shell Coulomb scattering amplitude, we derive the final expressions for the transfer matrix element in correspondence to different degrees of approximation for the core-core Coulomb scattering amplitude.

The initial and final state interactions will be formulated and discussed in terms of Feynman diagrams in Sect. 4. Finally, in Sect. 5 the FDA formulation is compared with the DWBA and TMA theories, and, in order to obtain some insight about the true reaction mechanism in the neutron transfer processes, we reformulate the problem in the framework of the general formal scattering theory.

2. - GENERAL OUTLINE OF THE FEYNMAN DIAGRAM APPROACH. -

The purpose of this Section is to introduce the non-relativistic Feynman diagram method, in a form suitable to be applied to heavy-ion transfer reactions.

The heavy-ion transfer reaction b(A, a)B can be represented schematically as:

$$(a+x)+b \to a+(b+x), \tag{2.1}$$

where a and b are the heavy nuclear "cores" of the nuclei A=a+x and B=b+x, and x is the particle (considered here to be a neutron), which is exchanged from one nucleus to the other, while the cores scatter in their mutual field.

Following Shapiro[3], we start from the assumption that the direct reaction amplitude $M_{fi}^{(o)}$, without taking into account the effects of the initial and final state interactions, is described by non-relativistic Feynman diagrams (with a small number of virtual particles). In selecting the most important Feynman graphs, one has to take into account both of the singularity positions and of the vertex function magnitudes.

In Fig. 1 the heavy-ion transfer amplitude $M_{fi}^{(o)}$ is expressed in terms of the amplitude of the simplest graphs, in which the particle x is transferred from the initial bound

state a+x to the final bound state b+x[x]. The small circles represent the three-ray vertex functions describing the virtual decay of A in a+x and the virtual syntesis of b+x in B. The small square represents the off-energy-shell core-core scattering amplitude.

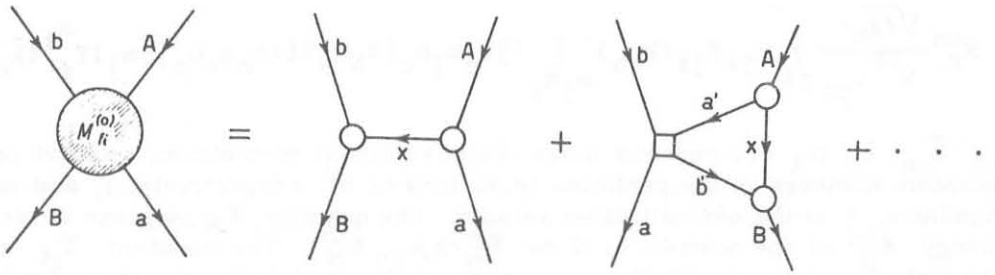

FIG. 1 - Diagram representation of the amplitude $M_{fi}^{(o)}$ for the transfer reaction b(A, a)B.

It is well known[3, 5] that the pole graph corresponds to the usual Butler mechanism. The form of its amplitude has been extensively studied in the literature. The triangular graph of Fig. 1 could appear of knock-on type; in effect it can be considered as a refinement of the pole mechanism: in addition to the neutron transfer the core-core interaction is taken into account. We devote the next Section to the analysis of its amplitude.

In order to obtain the direct reaction amplitude M_{fi} which describes also the initial and final state interaction effects, one can apply the diagram summation method (DSM)[6]. In this method the amplitude M_{fi} is constructed starting from the initial amplitude $M_{fi}^{(o)}$ by summing all the graphs which describe the initial and final channel interactions. This is accomplished in Fig. 2, where the shaded circle represents the amplitude $M_{fi}^{(o)}$, described by Fig. 1, and the small shaded squares represent the initial or final channel scattering amplitude.

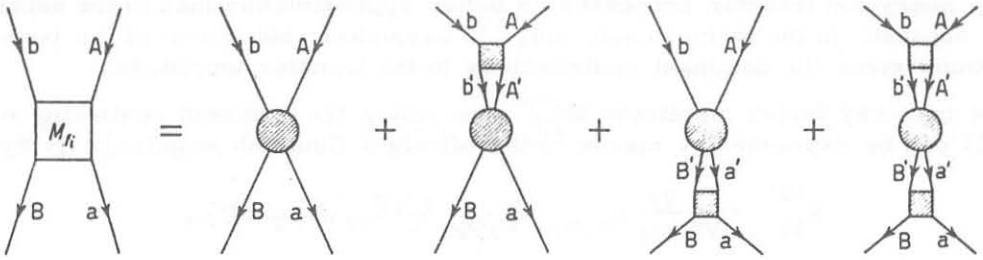

FIG. 2 - Diagram representation of the amplitude M_{fi} taking into account the initial and final state interactions.

According to the non-relativistic Feynman-diagram rules[3, 7], the amplitudes of the graphs which appear in Figs. 1 and 2 can be written in terms of the internal line propagators and of the three-ray and four-ray vertex functions. At energies below the Coulomb barrier, the four-ray vertices can be sufficiently well represented by the Coulomb scattering amplitude, because, owing to the strong repulsive Coulomb interactions, the nuclear potential effects are expected to be relatively unimportant. Among the nuclear interactions, only the neutron-core ones are taken into account. They are described by the three-ray vertex functions. Therefore, nuclear and Coulomb effects appear, in the reaction amplitude, into two different factors, the former in the neutron-core nuclear form factors, and the latter in the nucleus-core and core-core Coulomb scattering amplitudes.

(x) - The non-relativistic amplitude of graphs with two internal lines vanishes in our case. Triangular graphs corresponding to a cluster structure of A and B (or a and b) and quadrangular graphs describe mechanisms more complicated than neutron exchange; at low energies they would be inhibited by the strong Coulomb potential.

Let us consider the analytic expressions for the "vertex" functions. The three-ray vertex amplitude M_N^{cn} describing the virtual decay (or synthesis) of the nucleus N in (from) core + neutron state can be written, in the one-particle model[7,8], as:

$$(2.2)\qquad M_N^{cn}=\frac{\sqrt{2\chi_N}\pi}{V^{3/2}\mu_{cn}}\sum_{j\ell}\gamma_{j\ell}F_{j\ell}(k_{cn})\sum_{m_j m_\ell}(js_c m_j m_c|s_N m_N)(\ell s_n m_\ell m_n|jm_j)Y_\ell^{m_\ell}(\hat{k}_{cn})\ ,$$

where μ_{cn}, $\vec{k}_{cn}$; ℓ, m_ℓ are reduced mass, relative linear momentum, relative orbital momentum quantum numbers of the particles (c,n) (c=a or b), respectively; s_i and m_i are spin quantum numbers; V is the normalization volume. The quantity χ_N is given in terms of the binding energy ε_N^{cn} of the neutron in N by $\chi_N^2=2\mu_{cn}\varepsilon_N^{cn}$. The constant $\gamma_{j\ell}$ can be expressed through the reduced with $\theta_{j\ell}$, conventionally used in the direct nuclear reaction theories, and through a nuclear-surface radius R_N; one obtains:

$$|\gamma_{j\ell}|^2=\frac{6|\theta_{j\ell}|^2}{(\chi_N R_N)^3|h_\ell^{(1)}(i\chi_N R_N)|^2}$$

The nuclear form factor $F_{j\ell}(k_{cn})$ has the form:

$$(2.3)\qquad F_{j\ell}(k_{cn})=\frac{(k_{cn}^2+\chi_N^2)\int j_\ell(k_{cn}r)\phi_\ell(r)r^2dr}{\lim_{k_{cn}^2\to-\chi_N^2}\{(k_{cn}^2+\chi_N^2)\int j_\ell(k_{cn}r)\phi_\ell(r)r^2dr\}}\ ,$$

where $\phi_\ell(r)$ is the radial part of the bound-state wave function. The usual Wronskian form for the form factor (2.3), obtained at sufficiently small values of k_{cn}, represents, in the low-energy heavy-ion transfer processes, a better approximation than in the usual direct reactions, because, in the former case, only the asymptotic behaviour of the bound state wave functions gives the dominant contributions to the transfer amplitude.

The four-ray vertex amplitude $M_{12}^{1'2'}$ describing the Coulomb scattering of the particles (1,2) can be expressed by means of the off-shell Coulomb amplitude f_C by

$$(2.4)\qquad M_{12}^{1'2'}=\frac{1}{V^2}\frac{2\pi}{\mu_{12}}\delta_{m_1m_{1'}}\delta_{m_2m_{2'}}f_C(\vec{k}_{12},\vec{k}_{1'2'};E)\ ,$$

where μ_{12}, k_{12}, $k_{1'2'}$ and E are reduced mass, relative linear momentum before and after the scattering and center-of-mass kinetic energy of the particles (1,2) respectively. The amplitude f_C satisfies the generalized Lippman-Schwinger integral equation[10] and represents a regular function in the E variable with the exception of the physical energy spectrum[11]. The more useful form for f_C, together with its more used approximated expressions, will be introduced and discussed in Sec. 3.2.

3. - THREE-BODY REARRANGEMENT TRIANGULAR GRAPH MECHANISM. -

3.1. - General form for the triangular graph amplitude. -

We now consider the triangular graph introduced in the preceding Section. Let 1=a', 2=b', 3=n be the three internal virtual particles of the graph; $\vec{p}_i$, $\vec{p}_f$; ε_i, ε_f relative linear momenta and kinetic energies in the initial and final channels, respectively; $Q=\varepsilon_B^{23}-\varepsilon_A^{13}$ the reaction Q-value; μ_i, m_i, $\vec{k}_i$, E_i the mass, spin projection, linear momentum and kinetic energy of the i-particle in the center of mass system.

According to the well known non-relativistic Feynman rules, one obtains for the amplitude $M_{fi}(\Delta)$ of the triangular graph of Fig. 3

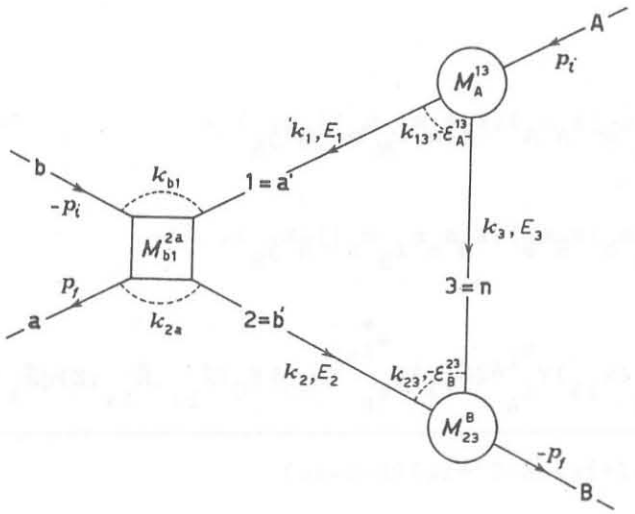

FIG. 3 - Three-body rearrangement triangular graph mechanism.

$$(3.1)\quad M_{fi}(\Delta) = -\frac{i}{(2\pi)^4} 8\mu_1\mu_2\mu_3 V^3 \sum_{m_1 m_2 m_3} \int \frac{M_A^{13} M_{23}^{B} M_{b1}^{2a} d\vec{k}_3 dE_3}{(k_1^2 - 2\mu_1 E_1 - i\varepsilon)(k_2^2 - 2\mu_2 E_2 - i\varepsilon)(k_3^2 - 2\mu_3 E_3 - i\varepsilon)},$$

where the vertex functions M_A^{13} (M_{23}^{B}) and M_{b1}^{2a} depend on the kinematic variables $\vec{k}_{13}(\vec{k}_{23})$; $\vec{k}_{b1}$, $\vec{k}_{2a}$ and E which are connected with the integration variables $\vec{k}_3$ and E_3 by the relations:

$$(3.2)\quad \vec{k}_{13} = \vec{k}_3 - \frac{\mu_n}{\mu_A}\vec{p}_i, \qquad \vec{k}_{23} = \vec{k}_3 + \frac{\mu_n}{\mu_B}\vec{p}_f, \qquad \vec{k}_{b1} = \vec{p}_i - \frac{\mu_b}{\mu_a+\mu_b}\vec{k}_3, \qquad \vec{k}_{2a} = \vec{p}_f + \frac{\mu_a}{\mu_a+\mu_b}\vec{k}_3,$$

$$E = \varepsilon_i - \varepsilon_A^{13} - E_3 - \frac{k_3^2}{2(\mu_a+\mu_b)} = \varepsilon_f - \varepsilon_B^{23} - E_3 - \frac{k_3^2}{2(\mu_a+\mu_b)} \quad ;$$

furthermore we obtain

$$(3.3)\quad \vec{p} = \vec{\Delta} - \vec{k}_3,$$

where $\vec{\Delta} = \vec{p}_i - \vec{p}_f$ is the momentum transfer in the reaction and $\vec{p} = \vec{k}_{b1} - \vec{k}_{2a}$ the momentum transfer in the core-core scattering.

By introducing in (3.1) the expressions (2.2) and (2.4) and changing the integration variable from E_3 to E, the amplitude $M_{fi}(\Delta)$ can be written, after suitable kinematic transformations,

$$(3.4)\quad M_{fi}(\Delta) = -\frac{i}{4\pi V^2} \frac{\sqrt{\chi_A \chi_B}}{\mu_{13}\mu_{23}\mu_{ab}} \sum_{\substack{j_A \ell_A m_{j_A} m_{\ell_A} \\ j_B \ell_B m_{j_B} m_{\ell_B}}} Y_{j_A \ell_A} Y_{j_B \ell_B} C^{m_{j_A} m_{\ell_A}}_{\substack{j_A \ell_A \\ j_B \ell_B}} C^{m_{j_B} m_{\ell_B}}_{\substack{m_{\ell_A} m_{\ell_B} \\ j_B \ell_B}} I^{(\Delta)}_{j_A \ell_A},$$

where

$$(3.5)\qquad C^{\,m_{j_A} m_{\ell_A}}_{\substack{j_A \ell_A \\ j_B \ell_B}} = (j_A s_a m_{j_A} m_a | s_A m_A)(\ell_A s_n m_{\ell_A} m_n | j_A m_{j_A}) \times$$

$$\times (j_B s_b m_{j_B} m_b | s_B m_B)(\ell_B s_n m_{\ell_B} m_n | j_B m_{j_B}),$$

$$(3.6)\qquad I^{\,m_{\ell_A} m_{\ell_B}}_{\substack{j_A \ell_A \\ j_B \ell_B}}(\Delta) = \int \frac{F_{j_A \ell_A}(k_{13}) F_{j_B \ell_B}(k_{23}) Y^{m_{\ell_A}}_{\ell_A}(\hat{k}_{13}) Y^{m^*_{\ell_B}}_{\ell_B}(\hat{k}_{23}) f_C(\vec{k}_{b1}, \vec{k}_{2a}; E) d\vec{k}_3 \, dE}{(E-T+i\varepsilon)(E-T'+i\varepsilon)(E-S-i\varepsilon)}$$

with

$$(3.7)\qquad T = \frac{k^2_{b1}}{2\mu_{ab}}, \quad T' = \frac{k^2_{2a}}{2\mu_{ab}}, \quad S = \varepsilon_i - \varepsilon^{13}_A - \frac{k^2_3}{2\mu_{3,(a+b)}}, \quad \mu_{3,(a+b)} = \frac{\mu_n(\mu_a+\mu_b)}{\mu_n+\mu_a+\mu_b}.$$

The integration over E of (3.6) can be performed in the complex E-plane. In fact, by putting $E+i\varepsilon = z$ and by choosing the integration path as in Fig. 4, since the contribution from the semicircle C_R vanishes in the limit $R \to \infty$, one obtains

$$\int_{-\infty}^{+\infty} \frac{f_C(\vec{k}_{b1}, \vec{k}_{2a}; E) dE}{(E-T+i\varepsilon)(E-T'+i\varepsilon)(E-S-i\varepsilon)} = 2\pi i \frac{f_C(\vec{k}_{b1}, \vec{k}_{2a}; S+i\varepsilon)}{(S-T+i\varepsilon)(S-T'+i\varepsilon)} .$$

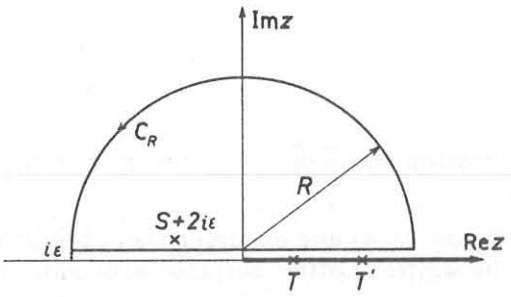

FIG. 4 - Integration path and singularities of the integrand function in (3.6), in the energy variable (x: poles, ——: cut).

By introducing this expression into (3.6), we have

$$(3.8)\qquad I^{\,m_{\ell_A} m_{\ell_B}}_{\substack{j_A \ell_A \\ j_B \ell_B}}(\Delta) = 2\pi i \int \frac{F_{j_A \ell_A}(k_{13}) F_{j_B \ell_B}(k_{23}) Y^{m_{\ell_A}}_{\ell_A}(\hat{k}_{13}) Y^{m^*_{\ell_B}}_{\ell_B}(\hat{k}_{23}) f_C(\vec{k}_{b1}, \vec{k}_{2a}; S) d\vec{k}_3}{(S-T)(S-T')}$$

where S includes a small positive imaginary part.

The equations (3.4) and (3.8) give the exact expression for the matrix element of the triangular graph represented in Fig. 3 and, by means of the well known relations presented

in Refs. (10, 12) they allow the evaluation of cross-sections for specific reactions. In order to go on, as far as possible, in the analytical integration and give an approximate evaluation of the cross-section behaviour corresponding to the considered mechanism, we will make these semplifying approximations.

a) First of all we observe that, for sufficiently heavy interacting ions, at low energies, recoil effects can be discarded; then one can put approximately

$$\vec{k}_{13} \approx \vec{k}_{23} \approx \vec{k}_3 .$$

Recoil corrections have been evaluated in specific models[13÷15].

b) Owing to the presence of oscillating factors in the Coulomb amplitude, the spherical harmonics can be brought out of the integral and calculated in correspondence of the saddle point Ω_0 in the angular variables[16,17]. This approximation is not necessary for zero orbital momenta.

From (3.4), by using the approximations (a) and (b) and carrying out the magnetic sums, one obtains

$$\sum_{\substack{m_b m_A \\ m_B m_a}} |M_{fi}(\Delta)|^2 =$$

$$= \frac{\chi_A \chi_B}{(8\pi V^2 \mu_{13}\mu_{23}\mu_{ab})^2} (2s_A+1)(2s_B+1) \sum_{\substack{j_A \ell_A \\ j_B \ell_B}} |Y_{j_A \ell_A}|^2 |Y_{j_B \ell_B}|^2 |J^{j_A \ell_A}_{j_B \ell_B}(\Delta)|^2 , \tag{3.9}$$

where

$$J^{j_A \ell_A}_{j_B \ell_B}(\Delta) = \int \frac{F_{j_A \ell_A}(k_{13}) F_{j_B \ell_B}(k_{23}) f_C(\vec{k}_{b1}, \vec{k}_{2a}; S) d\vec{k}_3}{(S-T)(S-T')} . \tag{3.10}$$

3.2.- General considerations on the Coulomb scattering amplitude.-

Let us first consider the problem of choosing the more convenient form for the Coulomb scattering amplitude to introduce in (3.10). The Coulomb problem has been discussed extensively by several authors[11, 18, 19], but it seems useful, at this point, to review some concepts and formulas on the argument.

The core-core Coulomb scattering appearing in the triangular graph of Fig. 3 can be described correctly by the complete off-energy-shell amplitude (generalized amplitude) which, in the forms derived by Schwinger[11], is written as

$$f_C(\vec{k}_{b1}, \vec{k}_{2a}; E) = -\frac{2\mu_{ab}\alpha}{p^2} + 2i\eta\mu_{ab}\alpha \int_0^1 \frac{\rho^{i\eta} d\rho}{\rho p^2 - \frac{\mu_{ab}}{2E}(E-T)(E-T')(1-\rho)^2} \tag{3.11a}$$

or

$$f_C(\vec{k}_{b1}, \vec{k}_{2a}; E) = \frac{\mu_{ab}^2 \alpha (E-T)(E-T')}{E} \int_0^1 \frac{\rho^{i\eta}(1-\rho^2) d\rho}{\left[\rho p^2 - \frac{\mu_{ab}}{2E}(E-T)(E-T')(1-\rho)^2\right]^2} \tag{3.11b}$$

where the so-called Sommerfeld parameter is given by $\eta = \alpha \sqrt{\frac{\mu_{ab}}{2E}}$ with $\alpha = Z_a Z_b e^2$.

If the energy E has a small positive imaginary part, (3.11a) can be expressed in terms of hypergeometric functions by the relation

$$f_C(\vec{k}_{b1},\vec{k}_{2a};E) = -\frac{2\mu_{ab}\alpha}{p^2} + \frac{4iE\eta\alpha}{(E-T)(E-T')(\rho_E^2-1)(1+i\eta)} \times \tag{3.12}$$

$$\times \left[F(1,1+i\eta;2+i\eta;\frac{1}{\rho_E}) - \rho^2 F(1,1+i\eta;2+i\eta;\rho_E)\right]$$

where:

$$\rho_E = \frac{(1+q)^{\frac{1}{2}}+1}{(1+q)^{\frac{1}{2}}-1}, \tag{3.13}$$

with

$$q = \frac{2\mu_{ab}(E-T)(E-T')}{Ep^2}. \tag{3.14}$$

The approximated expression of f_C for small off-energy-shell contributions can be derived from (3.12) for $|q| \ll 1$ ($\rho_E \approx 4/q$); one then obtains, after straightforward calculations:

$$f_C(\vec{k}_{b1},\vec{k}_{2a};E\sim T\sim T') = -\frac{\pi\eta_T \exp(-2i\sigma_0)}{\sinh(\pi\eta_T)}\left[\frac{(E-T)}{4T}\right]^{i\eta_T}\left[\frac{(T'-E)}{4T}\right]^{i\eta_T} f_{CR}(p) \tag{3.15}$$

where

$$f_{CR}(p) = \frac{2\mu_{ab}\alpha}{p^2}\left[\frac{8\mu_{ab}T}{p^2}\right]^{i\eta_T} \exp(2i\sigma_0) \tag{3.16}$$

represents the physical Coulomb scattering amplitude and

$$\eta_T = \alpha\sqrt{\frac{\mu_{ab}}{2T}}, \qquad \sigma_0 = \arg\left[\Gamma(1+i\eta_T)\right]. \tag{3.17}$$

In the approximation (3.15), the Sommerfeld parameter η can be considered approximately independent of E. On the other hand, (3.15) represents a good approximation as far as the off-energy-shell effects are effectively small in the region where the integral (3.10) receives the main contributions.

An energy-independent Sommerfeld parameter can appear in the amplitude only if both incoming (or outgoing) particles lie on the energy shell (see, for example, the graphs of Fig. 2). In this case the Coulomb scattering amplitude can be described by the expression (impulse approximation)

$$f_{CI}(\vec{k}_{b1},\vec{k}_{2a};E\sim T) = -\exp(-\tfrac{\pi}{2}\eta_T)\,\Gamma(1+i\eta_T)\left[\frac{T'-T-i\varepsilon}{4T}\right]^{i\eta_T} f_{CR}(\vec{k}_{b1},\vec{k}_{2a}), \tag{3.18}$$

which can be obtained from (3.12) for $E \to T+i\varepsilon$ ($T \neq T'$) and by dividing by the renormalization factor[19]

$$g = \exp(\tfrac{\pi}{2}\eta_T)\,\Gamma(1-i\eta_T)\left(\frac{E-T}{4T}\right)^{i\eta_T}.$$

We will return on this problem at the end of this Section.

3.3.- Triangular graph amplitude with generalized Coulomb scattering amplitude.-

For the calculation of the integral (3.10), it is more convenient to use the generalized scattering amplitude in the form (3.11b). By substituting (3.11b) in (3.10), one obtains:

$$J^{j_A \ell_A}_{j_B \ell_B}(\Delta) = J_G(\Delta) = \mu_{ab}^2 \alpha \int \frac{d\vec{k}_3}{S} F_{j_A \ell_A}(k_{13}) F_{j_B \ell_B}(k_{23}) \times$$

(3.19)

$$\times \int_0^1 \frac{\rho^{i\eta}(1-\rho^2)d\rho}{\left[\rho p^2 - \frac{\mu_{ab}}{2S}(S-T)(S-T')(1-\rho)^2\right]^2} ,$$

where S is given by (3.7) and the quantities S-T and S-T' can be related to the integration variables by

$$(3.20)\quad S-T = -\frac{1}{2\mu_{13}}(k_{13}^2+\chi_A^2) \approx -\frac{1}{2\mu_{13}}(k_3^2+\chi_A^2), \qquad S-T' = -\frac{1}{2\mu_{23}}(k_{23}^2+\chi_B^2) \approx -\frac{1}{2\mu_{23}}(k_3^2+\chi_B^2).$$

Performing the integral over the angular variables, one obtains

$$J_G(\Delta) = 4\pi\mu_{ab}^2\alpha \int_0^\infty \frac{F_{j_A \ell_A}(k_3) F_{j_B \ell_B}(k_3) k_3^2 dk_3}{S} \times$$

(3.21)

$$\times \int_0^1 \frac{\rho^{i\eta}(1-\rho^2)d\rho}{\left[\rho(\Delta+k_3)^2 - \frac{\mu_{ab}}{2S}(S-T)(S-T')(1-\rho)^2\right]\left[\rho(\Delta-k_3)^2 - \frac{\mu_{ab}}{2S}(S-T)(S-T')(1-\rho)^2\right]}$$

Introducing (3.21) in (3.9), one gets the modulus squared of the triangular graph matrix element when the core-core scattering is described by the generalized Coulomb amplitude. The integrals in (3.21) must be performed numerically; this calculation can be made rather easily, the only difficulty arising from the presence of the small imaginary part of S.

Looking at (3.21), one can see that, for $\varepsilon_i < \varepsilon_A^{13}$, the quantity S, given by (3.7), is negative in all the integration range of k_3. Then, the parameter $i\eta$ is real and positive (apart from a small positive imaginary part) and it goes to zero as $k_3 \to \infty$. The most important contributions to the integral (3.21) come from $k_3 \approx \Delta$ where the integral over ρ has a logarithmic-type divergency (for $\Delta \neq 0$). As $\Delta \to 0$ (forward scattering of the particles A and a, or backward scattering of the particles A and B), the main contributions come now from the region of small k_3-values, where the integrand function becomes large. Then, in this case, (3.21) gives a forward-peaked cross-section. For $\varepsilon_i > \varepsilon_A^{13}$, the parameter $i\eta$ is imaginary (apart from a small positive real part) up to the value $k_3^2 = 2\mu_{3,(a+b)}(\varepsilon_i - \varepsilon_A^{13})$. The strongly oscillating factor appearing in the integral could cancel the contributions for small k_3 values. In this case the cross-section could be backward-peaked.

In any case, owing to the complicate expression (3.21), definite conclusions on its detailed structure can be drawn only after suitable numerical calculations.

3.4.- Triangular graph amplitude for small off-energy shell contributions of the Coulomb amplitude.-

Now we will calculate the integral (3.10) with the Coulomb scattering amplitude described by the formula (3.15), corresponding to small off-energy-shell contributions. A discussion on the validity of this approximation will be made at the end of this Section. Furthermore, we will limit our considerations to the cases in which the two binding energies ε_A^{13} and ε_B^{23} are approximately equal.

Since in the region of validity of (3.15) k_3^2 is of the order of χ_A^2 or χ_B^2 with χ_A and χ_B sufficiently small, the main contributions come from the small k_3-values. Then

$$T=\frac{1}{2\mu_{ab}}(\vec{p}_i-\frac{\mu_b}{\mu_a+\mu_b}\vec{k}_3)^2\approx\varepsilon_i\ ;$$

and (3.15) becomes

$$(3.22)\qquad f_C(\vec{k}_{b1},\vec{k}_{2a};T)=-\frac{2\pi\mu_{ab}^{\alpha\eta}}{\operatorname{senh}(\pi\eta)}\exp(-\pi\eta)\left[\frac{\mu_{ab}}{8\varepsilon_i\mu_{13}\mu_{23}}\right]^{i\eta}\frac{(k_3^2+\chi_A^2)^{i\eta}(k_3^2+\chi_B^2)^{i\eta}}{(p^2)^{i\eta+1}}\ ,$$

where, now, η is constant: $\eta=\sqrt{\mu_{ab}/2\ \varepsilon_i}$. The formula (3.22) is similar to the Coulomb scattering amplitude used by Greider[1,20], apart from the factor $(k_3^2+\chi_A^2)^{i\eta}\times(k_3^2+\chi_B^2)^{i\eta}$, which takes into account the Coulomb field distortions during the interaction. Analogous expressions have been used also by other authors[21].

Introducing (3.22) in (3.10) and changing the integration variable from $\vec{k}_3$ to $\vec{p}$, one obtains:

$$(3.23)\qquad J_I(\Delta)=-\frac{16\pi^2\mu_{ab}\mu_{13}\mu_{23}^{\alpha\eta}}{\operatorname{senh}(\pi\eta)}\exp(-\pi\eta)\left(\frac{\mu_{ab}}{8\varepsilon_i\mu_{13}\mu_{23}}\right)^{i\eta}K(\Delta),$$

where

$$(3.24)\qquad K(\Delta)=\int_0^\infty\frac{dp}{p^{2i\eta}}\int_{-1}^{+1}\frac{d(\cos\theta_p)}{\left[(\vec{p}-\vec{\Delta})^2+\chi_A^2\right]^{1-i\eta}\left[(\vec{p}-\vec{\Delta})^2+\chi_B^2\right]^{1-i\eta}}\ .$$

In (3.24), the form factors are assumed equal to 1; this represents a good approximation for sufficiently small binding energies.

The integral (3.24) can be performed exactly in both variables for equal binding energies and written formally as (see Appendix)

$$(3.25)\qquad K(\Delta)=\frac{B(\frac{3}{2}-i\eta,\frac{1}{2}-i\eta)}{(\Delta^2+\chi^2)^{\frac{3}{2}-i\eta}}F(\tfrac{1}{2}-i\eta,\tfrac{3}{2}-i\eta,\tfrac{3}{2};\frac{\Delta^2}{\Delta^2+\chi^2}).$$

This expression gives, as (3.21), a forward-peaked cross-section.

The forward-backward ratio can be evaluated, in this case, using (I.4) and (I.5)

$$\left|\frac{J_I(\Delta=0)}{J_I(\Delta=\Delta_{max})}\right|^2\approx 32\eta^2\left(\frac{\Delta_{max}}{\chi}\right)^6.$$

For the reaction $^{14}N(^{14}N,^{13}N)^{15}N$ at ε_i=6 MeV, this ratio is equal to 10^6.

3.5.- Triangular graph amplitude using the on-energy-shell form for the Coulomb amplitude.-

By introdusing in (3.10) the form (3.16) for the Coulomb scattering amplitude, one obtains

$$J_R(\Delta)=16\pi\mu_{ab}\mu_{13}\mu_{23}\alpha(8\mu_{ab}\varepsilon_i)^{i\eta}\exp(2i\sigma_0)\int_0^{\infty}\frac{dp}{p^{2i\eta}}\int_{-1}^{+1}\frac{d(\cos\theta_p)}{\left[(\vec{p}-\vec{\Delta})^2+\chi_A^2\right]\left[(\vec{p}-\vec{\Delta})^2+\chi_B^2\right]},$$

with $T\approx\varepsilon_i$ and the form factors equal to 1. The integral on the left hand side can be performed analitically in both variables and gives, for equal binding energies:

$$J_R(\Delta)=\frac{8\pi^2\mu_{ab}\mu_{13}\mu_{23}\alpha(8\mu_{ab}\varepsilon_i)^{i\eta}\exp(2i\sigma_0)}{\cosh(\pi\eta)\ (\Delta^2+\chi^2)^{1+i\eta}}\times \tag{3.26}$$

$$\times\ \left\{\frac{1}{\chi}\cosh\left[\eta(\pi-2\operatorname{arctg}\frac{\chi}{\Delta})\right]+\frac{i}{\Delta}\operatorname{senh}\left[\eta(\pi-2\operatorname{arctg}\frac{\chi}{\Delta})\right]\right\}.$$

Formula (3.26) represents the well known expression for the matrix element derived by Greider in the TMA approach. It gives a backward peaked angular distribution, the forward-backward ratio being equal to:

$$\left|\frac{J_R(\Delta=0)}{J_R(\Delta=\Delta_{max})}\right|^2\approx\left(\frac{\Delta_{max}}{\chi}\right)^4 16\eta^2\exp\left[-2\eta(\pi-\frac{\chi}{p_i})\right].$$

For the reaction $^{14}N(^{14}N,^{13}N)^{15}N$ this value is equal to $3\cdot10^{-13}$ at ε_i=6 MeV.

3.6.- Validity of the approximations on the Coulomb amplitude and the role of the triangular graph mechanism.-

By inspection of the three relations (3.21), (3.23) and (3.26) one easily notices that their structures are very different. In order to compare the absolute values of these three expressions, we have calculated the quantity $|J(\Delta)|^2$ for $\Delta=0$ in (3.21) and (3.23), which give angular distributions forward peaked, and for $\Delta=\Delta_{max}$ in (3.26); one has, respectively,

$$|J_G(\Delta=0)|^2\approx1.4\times10^{9};\quad |J_I(\Delta=0)|^2\approx5.2\times10^{-34};\quad |J_R(\Delta=\Delta_{max})|^2\approx2.5\times10^{3};$$

where the calculations refer to the reaction $^{14}N(^{14}N,^{13}N)^{15}N$ for ε_i=6 MeV.

The very strong difference between $|J_G|^2$ and $|J_I|^2$, although surprising, can be explained and mainly attributed to two reasons. First of all, we remember that the Coulomb amplitude in the form (3.15) has been obtained from the generalized one for small values of the quantity q, given by (3.14). This condition is not satisfied for the reaction $^{14}N(^{14}N,^{13}N)^{15}N$, where the minimum q-value is approximately equal to 1 in the region of small k_3-values. Furthermore, as already mentioned, for $\varepsilon_i<\varepsilon_A$, the quantity S is negative everywhere in the k_3-range of integration; for this reason the assumption $S\approx T\approx\varepsilon_i$ is never verified and the Sommerfeld parameter η becomes a negative imaginary quantity. This follows from the fact that, for $\varepsilon_i<\varepsilon_A$ the two cores interact off-energy-shell at negative energies, even if the neutron is transferred at rest. On the contrary, since the position $S\approx T\approx\varepsilon_i$ implies a real and positive parameter η in $|J_I|^2$, the cross-section in the approximation of taking into account only small off-energy-shell contributions is strongly reduced by exponentially decreasing factors, and this approximation becomes meaningless.

In spite of the fact that the expression (3.26) gives a backward peaked angular distribution, the use of the Coulomb amplitude in the physical form, appears in this model hardly justifiable; especially in the case of heavy-ion interactions, where off-energy shell Coulomb distortions are important. In particular, the introduction of a real Sommerfeld parameter for the

core-core interaction is still incorrect. One can easily realize that the strong difference between the formula (3.26) and (3.21), and between the absolute values of the corresponding matrix elements are essentially due to: (a) the elimination in (3.26) of important oscillating factors, due to the Coulomb distortions; (b) the introducing of a constant and real η-parameter, used, normally, in the impulsive Coulomb amplitude for initial or final state interactions.

We notice that the triangular graph alone cannot represent correctly the overall process. In fact, the strong Coulomb interaction in the initial and final channels cannot in any case be neglected. The triangular graph must be considered as a tool for describing the transfer mechanism more correctly than in the DWBA and MSA theories, that use a simple pole graph. By adding to the triangular graph mechanism the initial and final state interactions, one can then obtain the correct behaviour of the angular distribution. On the other side, in order to obtain reliable nuclear information, it is necessary to describe correctly the transfer mechanism, because it includes those quantities which depend on nuclear structure. In this regard we remark that, the TMA approach, provided that the core-core Coulomb interactions are treated correctly, can be considered rather as a suggestion for a more appropriate description of the fundamental mechanism than a complete treatment of the entire process.

In order to show the importance of the triangular graph as basic mechanism with respect to the polar one (used in the DWBA and MSA), we have evaluated the ratio at $\Delta = 0$ between the squares of the corresponding matrix elements

$$\sum_{\substack{m_b m_A \\ m_a m_B}} |M_{fi}(\Delta)|^2 \Big/ \sum_{\substack{m_b m_A \\ m_a m_B}} |M_{fi}(\text{pole})|^2 \approx \frac{|J_G(\Delta)|^2 \chi^4}{64\pi^2 \mu_n^2 \mu_{ab}^2} .$$

This ratio, for the reaction $^{14}N(^{14}N, ^{13}N)^{15}N$ is equal to ≈ 24. The predominant role of the triangular graph is due to presence of the strong core-core Coulomb interaction.

4. - INITIAL AND FINAL STATE INTERACTIONS IN THE FEYNMAN DIAGRAM FORMALISM. -

In this Section we will discuss in details the problem of initial and final state interactions for the case of the heavy-ion transfer reactions. According to the Feynman diagram technique, this will be accomplished by the so-called DSM method[6], which consists in summing all the graphs of Fig. 2. For energies sufficiently below the Coulomb barrier, the initial and final elastic scattering amplitudes can be well represented by the Coulomb matrix element alone, as it is suggested by the experimental results on the elastic scattering at low energies.

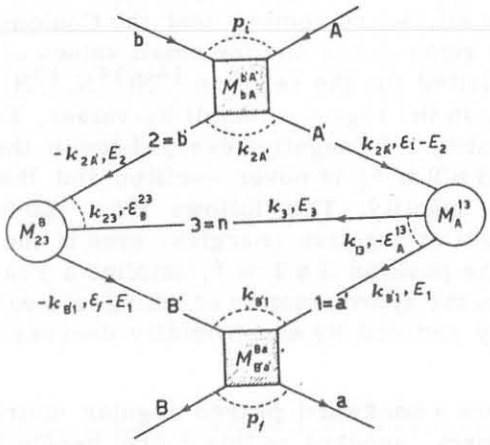

FIG. 5 - Initial and final state interactions on the basis of the pole graph.

As pointed out in Ref. (6), the matrix elements of the first three graphs on the right in Fig. 2 (if constructed on the basis of the pole graph) are respectively equal to the PWBA, DWBA with initial state interactions alone and DWBA with final state interactions alone; the only difference between the DSM and the complete DWBA theories arises from the term which corresponds to the fourth graph in Fig. 2. For this reason, we will now start by calculating the matrix element for the graph of Fig. 5.

By using the non-relativistic Feynman rules and integrating over the internal energies E_1 and E_2 by means of the residue method, one obtains:

$$M_{fi}=-\frac{4}{V^2\pi^2}\frac{\mu_a^2\mu_b^2\mu_n\mu_A\mu_B}{(\mu_A+\mu_b)^2\mu_{13}\mu_{23}\mu_{Ab}\mu_{aB}}\sqrt{\chi_A\chi_B}\times$$

(4.1)

$$\times\sum_{\substack{j_A\ell_A m_{j_A}m_{\ell_A}\\ j_B\ell_B m_{j_B}m_{\ell_B}}}\gamma_{j_A\ell_A}\gamma_{j_B\ell_B}C^{m_{j_A}m_{\ell_A}}_{j_A\ell_A\,m_{j_A}m_{\ell_A}}C^{m_{j_B}m_{\ell_B}}_{j_B\ell_B\,m_{j_B}m_{\ell_B}}I_{fi}\ ,$$

where

$$I_{fi}=$$

(4.2)

$$=\int\frac{F_{j_A\ell_A}(k_{13})F_{j_B\ell_B}(k_{23})Y_{\ell_A}^{m_{\ell_A}}(\hat{k}_{13})Y_{\ell_B}^{*m_{\ell_B}}(\hat{k}_{23})f_{CI}(\vec{p}_i,\vec{k}_{2A'};\varepsilon_i)f_{CI}(\vec{k}_{B'1},\vec{p}_f;\varepsilon_f)d\vec{k}_{2A'}d\vec{k}_{B'1}}{(k^2_{2A'}-p_i^2-i\varepsilon)(k^2_{B'1}-p_f^2-i\varepsilon)\frac{\mu_B}{\mu_b}\left[k^2_{23}+\chi_B^2+\frac{\mu_{23}}{\mu_{Ba}}(k^2_{B'1}-p_f^2)-i\varepsilon\right]}$$

The meaning of the kinematic symbols used in (4.1) and (4.2) appears in Fig. 5; they are mutually connected by the relations:

$$\vec{k}_{13}=\frac{\mu_a}{\mu_A}\vec{k}_{2A'}-\vec{k}_{B'1},\quad \vec{k}_{23}=\vec{k}_{2A'}-\frac{\mu_b}{\mu_B}\vec{k}_{B'1},\quad \vec{k}_3=\vec{k}_{2A'}-\vec{k}_{B'1}. \tag{4.3}$$

The matrix element in the complete DWBA theory can be obtained by neglecting the term $(\mu_{23}/\mu_{Ba})(k^2_{B'1}-p_f^2)$, appearing in the propagator in square bracket in (4.2), and adding to I_{fi} the contributions from the first three graphs in Fig. 2. If one takes into account the formulas (18), (A.1) and (A.2) of Ref. (19), one gets the complete factor I^c_{fi} to introduce in (4.1):

$$I^c_{fi}=\frac{\mu_b}{\mu_B}\pi^3\exp\left(-\frac{\pi}{2}(\eta_i+\eta_f)\right)Y_{\ell_A}^{m_{\ell_A}}(\Omega_0)Y_{\ell_B}^{*m_{\ell_B}}(\Omega_0)\,\Gamma(1+i\eta_i)\Gamma(1+i\eta_f)\int\exp\left(-i\frac{\mu_b}{\mu_B}\vec{p}_f\cdot\vec{r}\right)\times \tag{4.4}$$

$$\times\,F\left(-i\eta_f,1;i\frac{\mu_b}{\mu_B}\left[p_f r+\vec{p}_f\cdot\vec{r}\right]\right)\frac{\exp(-\chi_B r)}{r}\exp(i\vec{p}_i\cdot\vec{r})F\left(-i\eta_i,1;i\left[p_i r-\vec{p}_i\cdot\vec{r}\right]\right)d\vec{r}$$

where the spherical functions and form factors are approximated as in Sect. 3, and $\eta_i(\eta_f)$ is the Sommerfeld parameter in the initial (final) state.

The expression (4.4) corresponds to the matrix element obtained in the DWBA approach in the so-called "post" representation[12]. We remark that, in virtue of the equality:

$$\frac{\mu_b}{\mu_B}\left[k^2_{23}+\chi_B^2+\frac{\mu_{23}}{\mu_{Ba}}(k^2_{B'1}-p_f^2)\right]^{-1}=\frac{\mu_a}{\mu_A}\left[k^2_{13}+\chi_A^2+\frac{\mu_{13}}{\mu_{Ab}}(k^2_{2A'}-p_i^2)\right]^{-1}, \tag{4.5}$$

the matrix element of the so-called "prior" representation can be obtained in the same way, by starting from the propagator written as in the right side of (4.5) and by dropping the quantity $(\mu_{13}/\mu_{Ab})(k^2_{2A'}-p_i^2)$.

Since the presence of the term $\mu_{23}/\mu_{Ba})(k^2_{B'1}-p_f^2)$ in the exact propagator (4.5) reflects the existence of a three particle-cut, as shown in Ref. (6), one can say that the three--particle intermediate state (1, 2, 3) appearing in Fig. 5 eliminates the "post-prior" paradox of the DWBA. This represents a further reason for thinking the DSM a better ap-

proximation than the DWBA in treating the initial and final state interactions. The study of the role of the three particle-cut in (4.2) and the comparison of the two theories represents, however, an open problem, which would be useful to solve in order to obtain a more justifiable criterion of choice between "prior" and "post" representation.

We remark that one of the main features of the transfer reactions is that, for sufficiently heavy particles, nuclear interactions can be considered as a small perturbation of the strong Coulomb scattering. For this reason, the main term of both the DSM and the DWBA theories would be represented by (4.2) (in the DWBA the three-particle cut is neglected), which is quadratic in the Coulomb scattering amplitude[1].

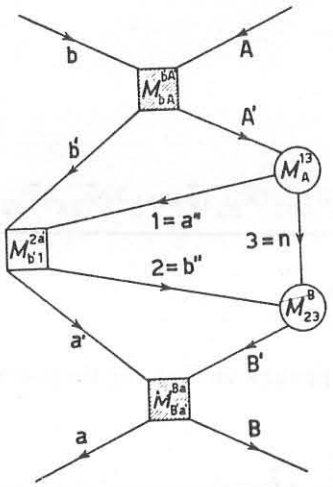

FIG. 6 - Triangular graph mechanism with initial and final state interactions.

The same technique can be used for describing the initial and final interactions starting from the triangular graph of Fig. 3 we proposed in the preceding Section. This is accomplished in Fig. 6, where the important Coulomb interactions are correctly represented in the initial, intermediate and final state. The evaluation of the cross-sections, coming from this graph, is in progress in some practical cases.

5. - COMPARISON OF FDA, TMA AND DWBA THEORIES. -

The exact transition matrix element M_{fi} for the rearrangement scattering (a+n)+b → a+(b+n) can be derived from the formal scattering theory. We would like to write two exact expressions for M_{fi}, which will be suitable for the comparison of DWBA and TMA approaches with the FDA theory.

Let H_a and H_b be the hamiltonians for the internal structure of the two systems a and b respectively; K_a, K_b and K_n the kinetic energy operators for the center-of-mass motion of the systems a, b and n; V_{an}, V_{bn} and V_{ab} the interactions between the systems (a,n) (b,n) and (a,b). The initial and final channel hamiltonians K_i and K_f and the channel interactions V_i and V_f are then:

$$(5.1)\qquad K_i=K+H+V_{an}\ ,\quad K_f=K+H+V_{bn}\ ,\qquad (5.2)\qquad V_i=V_{ab}+V_{bn}\ ,\quad V_f=V_{ab}+V_{an}\ ,$$

where $K=K_a+K_b+K_n$ and $H=H_a+H_b$. The complete hamiltonian is:

$$(5.3)\qquad \mathcal{H}=K_i+V_i=K_f+V_f\ .$$

Let now Φ_i and Φ_f be the initial and final channel wave functions and $\Psi_i^{(+)}$ and $\Psi_f^{(-)}$ the wave functions describing the entire scattering process and asymptotic to Φ_i and Φ_f, respectively. The scattering matrix is:

$$(5.4)\qquad M_{fi}=(\Phi_f,(V_{ab}+V_{an})\Psi_i^{(+)})=(\Psi_f^{(+)},(V_{ab}+V_{bn})\Phi_i)\ .$$

Now, introducing the partially interacting states

$$(5.5)\qquad \chi_{iD}^{(+)}=\left[1+\frac{1}{E_i-(K_i+V_{ab})+i\varepsilon}V_{ab}\right]\Phi_i\ ,\quad \chi_{fD}^{(-)}=\left[1+\frac{1}{E_f-(K_f+V_{ab})-i\varepsilon}V_{ab}\right]\Phi_f\ ,$$

and

$$(5.6)\qquad \chi_{iT}^{(+)}=\left[1+\frac{1}{E_i-(K_i+V_{bn})+i\varepsilon}V_{bn}\right]\Phi_i\ ,\quad \chi_{fT}^{(-)}=\left[1+\frac{1}{E_f-(K_f+V_{an})-i\varepsilon}V_{an}\right]\Phi_f$$

where $E_i=\varepsilon_i-\delta_A-\delta_b$, $E_f=\varepsilon_f-\delta_B-\delta_a$, with δ_j the total binding energy of the j-particle, and following the treatment of the two-potential problem for the rearrangement scattering as given by Goldberger and Watson[22], we obtain, in the limit $\varepsilon\to 0^+$,

(5.7) $$M_{fi}=\left(\chi_{fD}^{(-)},\left(V_{bn}+V_{an}\frac{1}{E_i-\mathcal{H}+i\varepsilon}V_{bn}\right)\chi_{iD}^{(+)}\right),$$

by using (5.5) and

(5.8) $$M_{fi}=\left(\chi_{fT}^{(-)},\left(V_{ab}+V_{ab}\frac{1}{E_i-\mathcal{H}+i\varepsilon}V_{ab}\right)\chi_{iT}^{(+)}\right),$$

by using (5.6). We notice that the terms $\left(\Phi_f,(V_{ab}+V_{an}-V_{bn})\chi_{iD}^{(+)}\right)$ and $\left(\Phi_f,V_{an}\chi_{iT}^{(+)}\right)$ vanish in the limit $\varepsilon\to 0^+$. Therefore the question of neglecting them does not arises[1,20,21]. Both (5.7) and (5.8) are exact expressions for the M-matrix element and represent the starting point for introducing the DWBA and TMA theories, respectively.

The partially interacting states (5.6) are pure nuclear states, while the partially interacting states (5.5) become pure Coulomb states below the Coulomb barrier.

The DWBA approach can be obtained from (5.7): (a) by keeping only the operator V_{bn} in the bracket; (b) by replacing the wave functions $\chi_{iD}^{(+)}$ and $\chi_{fD}^{(-)}$ by the corresponding $\chi_{fDW}^{(+)}$ and $\chi_{fDW}^{(-)}$ which describe the elastic scattering in the initial and final state channels (optical distorted wave functions):

(5.9) $$M_{fi}^{DWBA}=\left(\chi_{fDW}^{(-)},V_{bn}\chi_{iDW}^{(+)}\right)$$

The TMA approximation at low energies can be obtained from (5.8): (a) by replacing the operator in the bracket by means of the two body U_C operator for the off-energy-shell Coulomb scattering; (b) by using the plane wave Φ_i, Φ_f instead of $\chi_{iT}^{(+)}$ and $\chi_{fT}^{(-)}$

(5.10) $$M_{fi}^{TMA}=(\Phi_f,U_C\Phi_i).$$

In the practical calculations the on-energy-shell form is assumed for the Coulomb operator U_C.

The two formulations appear to be rather different. In fact, while in the DWBA the strong Coulomb interactions are correctly treated in the initial and final state and are completely neglected in the intermediate states, the TMA approximation, derived from a less intuitive form for the exact matrix element, gives a good account of the Coulomb interactions in the intermediate states, but does not allow a simple understanding of the initial and final interaction effects.

Let us now look for a formal theory representation of the fundamental mechanism amplitude $M_{fi}(\Delta)$. After introducing (2.4) in the $M_{fi}(\Delta)$ and integrating over the energy, we obtain by means of (3.3) and (3.20).

(5.11) $$M_{fi}(\Delta)=-\frac{V}{\pi^2}\frac{\mu_{13}\mu_{23}}{\mu_{ab}}\sum_{m_3}\int\frac{M_A^{13}M_{23}^B f_C(\vec{p})d\vec{p}}{(k_{13}^2+\chi_A^2)(k_{23}^2+\chi_B^2)}.$$

Introducing the Fourier transform of $f_C(\vec{p})=f_C(\vec{k}_{b1},\vec{k}_{2a};S)$

(5.12) $$f_C(\vec{p})=-\frac{\mu_{ab}}{2\pi}\int\exp(i\vec{p}\cdot\vec{r}_{ba})\phi_C(\vec{r}_{ba})d\vec{r}_{ba},$$

and rewriting the nuclear vertex functions M_N^{cn} in the form

(5.13) $$M_N^{cn}=\frac{1}{2\mu_{cn}V^{3/2}}\sum_{j\ell}\beta_{j\ell}\sum_{m_j m_\ell}(\ell s_n,m_\ell m_n|jm_j)(js_c,m_j m_c|s_N m_N)\times$$
$$\times(k_{CN}^2+\chi_N^2)\int\exp(-i\vec{k}_{cn}\cdot\vec{r})\phi_\ell(r)Y_\ell^{m_\ell}(\hat{r})d\vec{r},$$

where the quantity $\beta_{j\ell}$ is connected with the $\gamma_{j\ell}$ one by the relation

$$\beta_{j\ell}=\gamma_{j\ell}\sqrt{\frac{\chi_N}{2}}(-i)^{-\ell}\left[\lim_{k_{cn}^2\to-\chi_N^2}\{(k_{cn}^2+\chi_N^2)\int j_\ell(k_{cn}r)\phi_\ell(r)r^2dr\}\right]^{-1}, \tag{5.14}$$

the amplitude (5.11) becomes:

$$M_{fi}(\Delta)=\frac{1}{8\pi^3V^2}\sum_{\substack{j_A\ell_Am_{j_A}m_{\ell_A}\\ j_B\ell_Bm_{j_B}m_{\ell_B}}}\beta_{j_A\ell_A}\beta_{j_B\ell_B}C^{m_{j_A}m_{\ell_A}\ m_{j_B}m_{\ell_B}}_{j_A\ell_A\ j_B\ell_B}\ I_r\ , \tag{5.15}$$

where

$$I_r=\int\exp(i\vec{k}_{23}\cdot\vec{r}_{23})\phi^*_{\ell_B}(r_{23})Y^{m_{\ell_B}*}_{\ell_B}(\hat{r}_{23})\exp(i\vec{p}\cdot\vec{r}_{ba})\times$$
$$\times\ \varrho_C(\vec{r}_{ba})\exp(-i\vec{k}_{13}\cdot\vec{r}_{13})\phi_{\ell_A}(r_{13})Y^{m_{\ell_A}}_{\ell_A}(\hat{r}_{13})d\vec{r}_{23}d\vec{r}_{ba}d\vec{r}_{13}d\vec{p}\ , \tag{5.16}$$

with the co-ordinate vectors $\vec{r}_{13}$, $\vec{r}_{23}$ and $\vec{r}_{ba}$ defined in Fig. 7 and mutually connected among them and with $\vec{r}_i$ and $\vec{r}_f$ by the realtions

$$\vec{r}_i\equiv\vec{r}_{bA}=\vec{r}_{ba}+\frac{\mu_n}{\mu_A}\vec{r}_{13},\quad \vec{r}_f\equiv\vec{r}_{Ba}=\vec{r}_{ba}-\frac{\mu_n}{\mu_B}\vec{r}_{23},\quad \vec{r}_{23}=\vec{r}_{ba}+\vec{r}_{13}. \tag{5.17}$$

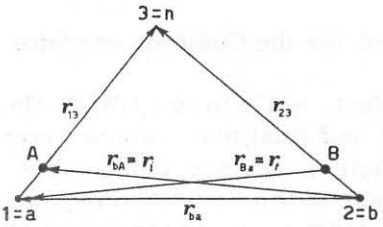

FIG. 7 - The system of coordinate vectors.

By taking into account the kinematic relations (3.2) and the vectors transformation (5.17), the integration over the $\vec{p}$ and $\vec{r}_{23}$ variables can be easily performed; it results

$$M_{fi}(\Delta)=\frac{1}{V^2}\sum_{\substack{j_A\ell_Am_{j_A}m_{\ell_A}\\ j_B\ell_Bm_{j_B}m_{\ell_B}}}\beta_{j_A\ell_A}\beta_{j_B\ell_B}C^{m_{j_A}m_{\ell_A}\ m_{j_B}m_{\ell_B}}_{j_A\ell_A\ j_B\ell_B}\int\exp(-i\vec{r}_f\cdot\vec{p}_f)\phi^*_{\ell_B}(r_{23})Y^{m_{\ell_B}*}_{\ell_B}(\hat{r}_{23})\times$$
$$\times\ \phi_C(\vec{r}_{ba})\exp(i\vec{r}_i\cdot\vec{p}_i)\phi_{\ell_A}(r_{13})Y^{m_{\ell_A}}_{\ell_A}(\hat{r}_{13})d\vec{r}_{ba}d\vec{r}_{13}. \tag{5.18}$$

The Lippmann-Schwinger integral equation satisfied by the matrix element $f_C(\vec{p})$ (6,10) is equivalent to the formal expression for the operator W_C

$$W_C=V_{ab}+V_{ab}\ \frac{1}{S-(K_{ab}+V_{ab})+i\varepsilon}V_{ab}, \tag{5.19}$$

where K_{ab} is the kinetic-energy operator for the core-core relative motion.

It is easy to see that the Green operator

$$\left[S-(K_{ab}+V_{ab})+i\varepsilon\right]^{-1} \quad \text{can be replaced by} \quad \left[E_i-(K+H+V_{ab})+i\varepsilon\right]^{-1},$$

when applied to the channel states Φ_i and Φ_f, containing eigenstates describing the internal structure of a and b systems. In fact, the operator K+H can be written (in the barycentric subspace) as:

$$K+H=K_{ab}+K_{n,(a+b)}+H_a+H_b$$

where $K_{n,(a+b)}$ is the kinetic energy operator for the neutron-(a+b) center of mass relative motion. When applied to the channel states Φ_i and Φ_f, the term $K_{n,(a+b)}+H_a+H_b$ gives the correct quantity $\left[k_3^2/2\mu_{3,(a+b)}\right] - \delta_a - \delta_b$, which must be added to S in order to obtain E_i.

Finally, from (5.18) and (5.19) we can write the desired formal expression for the $M_{fi}(\Delta)$

$$M_{fi}(\Delta)=\left(\phi_f,(V_{ab}+V_{ab}\frac{1}{E_i-(K+H+V_{ab})+i\varepsilon}V_{ab})\phi_i\right). \tag{5.20}$$

This result can be intuitively understood. In fact, in the intermediate state, there is only the core-core interaction V_{ab} and the intermediate state hamiltonian K_m has the form

$$K_m=K+H+V_{ab}=\mathcal{H}-V_{an}-V_{bn},$$

which is symmetric with respect to the initial and final state.

Equation (5.20) can be derived from (5.8) by neglecting all nuclear interactions both in the operators and in the states $\chi^{(-)}_{iT}$ and $\chi^{(-)}_{fT}$. We remark that the intermediate state core-core Coulomb interactions are contained in the latter term of the exact matrix element (5.7), which is completely neglected in the DWBA theory. The three-triangle graph of figure 6 we proposed represents a simple and very reasonable physical way for taking into account the Coulomb effects of this latter term, whose absolute value, as mentioned at the end of Sect. 3, would be larger than the one in the DWBA. We hope that a correct treatment of the graph of Fig. 6 can give, besides a reasonable agreement with both the angular and energy experimental distributions, reliable nuclear structure information.

We wish to thank Professor C. Villi for his fruitful suggestions and constant encouragement throughout the work.

APPENDIX

In the case of equal binding energies, the integral (3.24) can be directly integrated on the angular variable $\cos\theta_p$ and then it becomes

$$K(\Delta)=\int_0^\infty \frac{dp}{p^{2i\eta}}\int_{-1}^{1}\frac{d(\cos\theta_p)}{\left[(\vec{p}-\vec{\Delta})^2+\chi^2\right]^{2-2i\eta}}=\frac{1}{(2i\eta-1)\,2\Delta(\Delta^2+\alpha^2)^{1-i\eta}}\times \tag{A.1}$$

$$\times\left\{\int_0^\infty x^{-2i\eta-1}\left[(x^2+2x\cos t+1)^{1-2i\eta}-(x^2+2x\cos(\pi-t)+1)^{1-2i\eta}\right]dx\right.$$

where $\cos t = \Delta/\sqrt{\Delta^2+\chi^2}$.

Adding to η a small imaginary part and using (3.252.10) of Ref. (23), one obtains

$$K(\Delta)=\frac{2^{\frac{1}{2}-2i\eta}(\operatorname{sen}t)^{-\frac{1}{2}+2i\eta}\Gamma(\frac{3}{2}-2i\eta)B(-2i\eta,2-2i\eta)}{2\,(2i\eta-1)\Delta(\Delta^2+\chi^2)^{1-i\eta}}\left[P_{\frac{1}{2}}^{-\frac{1}{2}+2i\eta}(\cos t)-P_{\frac{1}{2}}^{-\frac{1}{2}+2i\eta}(\cos t)\right]. \tag{A.2}$$

This last expression can be putted in a more convenient form in terms of the hypergeometric functions. Using (15.4.26) of Ref. (24) one gets

$$K(\Delta)=\frac{1}{(\Delta^2+\chi^2)^{\frac{3}{2}-i\eta}}B(\tfrac{3}{2}-i\eta,\tfrac{1}{2}-i\eta)F(\tfrac{1}{2}-i\eta,\tfrac{3}{2}-i\eta,\tfrac{3}{2};\frac{\Delta^2}{\Delta^2+\chi^2}). \tag{A.3}$$

For $\Delta = 0$ (forward scattering) (A.3) becomes

$$K(\Delta=0)=\chi^{2i\eta-3}B(\tfrac{3}{2}-i\eta;\tfrac{1}{2}-i\eta), \tag{A.4}$$

while, for $\Delta \gg \chi\ \left[\Delta^2/(\Delta^2+\chi^2)\sim 1\right]$ (backward scattering) (A.3) gives

$$K(\Delta>>\chi)=\frac{\sqrt{\pi}}{2}\Delta^{2i\eta-3}B(\tfrac{3}{2}-i\eta,\tfrac{1}{2}-i\eta)\frac{\Gamma(2i\eta-\frac{1}{2})}{\Gamma(i\eta)\Gamma(1+i\eta)}\ . \tag{A.5}$$

REFERENCES. -

(1) - K.R. Greider, Adv. Theor. Phys. 1, 245 (1965).
(2) - K.R. Greider, Ann. Rev. Nuclear Sci. 15, 251 (1965).
(3) - I.S. Shapiro, Selected Topics in Nuclear Theory (Vienna 1963), p. 85.
(4) - L.D. Blokhintsev, E.I. Dolinskii and V.S. Popov, Nuclear Phys. 40, 117 (1963).
(5) - H.J. Schnitzer, Revs. Modern Phys. 37, 666 (1965).
(6) - E.I. Dolinskii, L.D. Blokhintsev and A.M. Mukhamedzhanov, Nuclear Phys. 76, 289 (1966).
(7) - I.S. Shapiro and S.F. Timashev, Nuclear Phys. 79, 46 (1966).
(8) - L. Taffara and V. Vanzani, Nuovo Cimento 56 B, 166 (1968).
(9) - P. Beregi, V.G. Neudatchin and Yu F. Smirnov, Nuclear Phys. 60, 305 (1964).
(10) - L. Taffara and V. Vanzani, Nuovo Cimento 52 B, 570 (1967).
(11) - J. Schwinger, J. Math. Phys. 5, 1606 (1964).
(12) - P.J.A. Buttle and L.J.B. Goldfarb, Nuclear Phys. 78, 409 (1966).
(13) - L.R. Dodd and K.R. Greider, Phys. Rev. Letters 14, 959 (1965).
(14) - T. Sawaguri and W. Tobocman, J. Math. Phys. 8, 2223 (1967).
(15) - L. Taffara and V. Vanzani, Nuovo Cimento 57 B, 229 (1968).
(16) - K.A. Ter-Martirosyan, Soviet Phys.-JETP 2, 620 (1956).
(17) - A. Dar, A. De-Shalit and A.S. Reiner, Phys. Rev. 131, 1732 (1963); A. Dar, Phys. Rev. 139 B, 1193 (1965).
(18) - S. Okubo and D. Feldman, Phys. Rev. 117, 292 (1960); W.F. Ford, Phys. Rev. 133 B, 1616 (1964); L. Hostler, Journ. Math. Phys. 5, 591, 1235 (1964).
(19) - E.I. Dolinskii and A.M. Mukhamedzhanov, Soviet J. Nuclear Phys. 3, 180 (1966).
(20) - K.R. Greider, Phys. Rev. 133 B, 1483 (1964).
(21) - J. Perrenoud and E. Sheldon, Nuclear Phys. A 102, 105 (1967).
(22) - M.L. Goldberger and K.M. Watson, Collision Theory (New York, 1964), p. 838.
(23) - I.S. Gradshteyn and I.M. Ryzhik, Tables of Integrals, Series and Products (New York, 1965).
(24) - M. Abramowitz and I.A. Stegun, Handbook of Mathematical Functions (New York, 1965).